1. Mohamed FAWZY[1], 2. Hani ATTAR[2], 3. Ayman AMER[2], 4. Sameh ALSAQOOR[3,4], 5. Ali ALAHMER[4,5], 6. Gabriel BOROWSKI[6], 7. Ahmed A.A. SOLYMAN[7], 8. Samer AS'AD[8], 9. Ramy Said AGIEB[1]

MTI University, Cairo, Egypt (1), Zarqa University, Zarqa, Jordan (2), Applied Science Private University, Amman, Jordan (3), Tafila Technical University, Tafila, Jordan (4), Tuskegee University, Tuskegee, United States of America (5), Lublin University of Technology,
Lublin, Poland (6), Glasgow Caledonian University, Glasgow, UK (7), Middle East University, Amman, Jordan (8).
ORCID: 1. 0000-0002-7088-840X; 2. 0000-0001-8028-7918; 3. 0000-0002-7693-5617; 4. 0000-0002-0552-8926; 5. 0000-0002-2994-1504; 6. 0000-0001-6971-5395; 7. 0000-0002-2881-8635; 8. 0000-0003-4127-3286; 9. 0000-0002-3113-017X

doi:10.15199/48.2024.04.60

Comparison of the Performance of PID and TVLQR Controllers for Nonlinear Modelling of a Freedom Flying Body

Abstract. *The aim of the research was to enhance the trajectory control of a nonlinear freedom flying body model by comparing time-varying linear quadratic regulator (TVLQR) controller with proportional–integral–derivative (PID) control. The nonlinear behavior of the flying body is represented using a linear time-varying (LTV) approach, accounting for parameter variations over time. The equations of motion for the LTV model and the nonlinear flying body were elaborated within the Matlab-Simulink environment. The optimization method was utilized to adapt the PID gains for the simulation of the nonlinear flying body. Their response was then compared to that of identical PID gains implemented on the LTV model. TVLQR optimal controller was generated by solving the Riccati Equation. A comparison between the performance of TVLQR and PID controllers was conducted using a nonlinear flying body. Additionally, the study examined the impact of wind by introducing wind velocity to the velocity of the flying body. In conclusion, we found that the TVLQR controller had better tracking performance, it excelled in actuator deflection, was wind resistant, and effectively dealt with dynamics and actuator uncertainties.*

Streszczenie. *Celem badań było usprawnienie kontroli trajektorii nieliniowego modelu swobodnie latającego obiektu poprzez porównanie regulatora zmiennoprzecinkowego liniowego regulatora kwadratowego (TVLQR) ze sterowaniem proporcjonalno-całkująco-różniczkującym (PID). Nieliniowe zachowanie latającego obiektu przedstawiono za pomocą modelu liniowego zależnego od czasu (LTV), uwzględniającego zmiany parametrów w czasie. Równania ruchu modelu LTV oraz nieliniowego obiektu latającego opracowano w środowisku Matlab-Simulink. Zastosowano metodę optymalizacji w celu dostosowania wzmocnień PID do symulacji nieliniowego obiektu latającego. Ich odpowiedź została następnie porównana z identycznymi wzmocnieniami PID zastosowanymi w modelu LTV. Optymalny kontroler TVLQR został wygenerowany poprzez rozwiązanie równania Riccatiego. Porównanie wydajności regulatorów TVLQR oraz PID przeprowadzono przy użyciu nieliniowego obiektu latającego. W pracy zbadano ponadto wpływ wiatru poprzez wprowadzenie prędkości wiatru do prędkości przemieszczającego się obiektu latającego. W podsumowaniu stwierdzono, że sterownik TVLQR miał lepszą wydajność śledzenia obiektu, wyróżniał się pod względem odchylenia siłownika, był odporny na wiatr i skutecznie poradził sobie z dynamiką i niepewnością siłownika.* **(*Porównanie wydajności kontrolerów PID i TVLQR do modelowania nieliniowego obiektu swobodnie latającego*)**

Keywords: PID controller, TVLQR controller, nonlinear modelling, freedom flying body
Słowa kluczowe: regulator PID, regulator TVLQR, modelowanie nieliniowe, obiekt swobodnie latający

Introduction

The increasing complexity of factories and the heightened standards in complicate manufacturing have driven a growing demand for automated control systems. The utilization of the 6-degree-of-freedom (6-DOF) missile model is crucial for obtaining precise insights into the missile's trajectory. TVLQR optimal control is established by leveraging the linear time-varying (LTV) model, which obtains a time-varying state feedback gain through an online solution of the Riccati Equation. This TVLQR optimal control, derived from the LTV model, is then applied to the nonlinear dynamics of the missile in the pitch channel. Additionally, the TVLQR controller is equipped to accommodate pitch angle limits for actuators.

According to MacKenzie, guiding can be defined as the process of steering a moving object towards a predetermined destination [1]. Draper provided insight by explaining that guidance relies on fundamental principles and encompasses comparable systems for guiding vehicles across a range of environments, not limited to our atmosphere, including gravitational fields and space [2]. The term "guided missile" identifies the most affluent and prepared entity for steering. It denotes an unmanned spacecraft capable of autonomously managing its trajectory [3]. In modern missile control methodologies, various guidance techniques are employed, such as classical control, optimal control, fuzzy logic, neural network control, differential geometric control strategies, and control principles based on differential game theory. Additionally, Elbes [4] and Westrum [5] provide a clear and comprehensive overview of the advancement in steering missile techniques.

The application of constructional control, especially the concept of optimal control, has been a subject of extensive research in recent decades. However, traditional control algorithms rely on conventional methods, and researchers have recognized that implementing the linear quadratic regulator (LQR) faces limitations in terms of resources for constructional application [6, 7]. The LQR method is a widely recognized approach, and its principles have been extended to encompass the framework of nonlinear control and nonlinear models [8, 9]. The formula developed by Wu et al. [10] included the energy component of a single earthquake but did not ensure the optimal response to subsequent earthquakes. Ayman et al. [11] introduced a predictor-corrector technique with applications aimed at constructing isolated systems to address the challenge of optimal control. Utilizing the LQR approach, this method simplifies the process, bypassing the need for intricate, time-consuming work, and yields control structures better suited for integration into a missile's onboard computer [12, 13].

The goals of this study were: (1) establish an advanced mathematical model for simulating the flight path of a free body within the pitch channel as a shared algorithm for designing, analysing, and enhancing the framework responsible for controlling via Simulink; and (2) evaluate the effectiveness of the proposed model, which incorporates a time-varying linear quadratic regulator (TVLQR) control technique to tackle the challenge of flying body attitude control, considering system characteristics and the specific demands of the application environment [14].

The mathematical model of 6-DOF flying body

The model encompasses 6-DOF equations, categorized into four distinct groups: dynamics (comprising gravity, aerodynamic, and thrust factors), kinematics, autopilot (which includes instruments, electronics, and actuators), and a prominent guidance descent model. The model's input includes parameters such as situational data, target trajectory, and target motion, while the outputs characterize the missile's flight behavior, including aspects like attitude angles, missile velocity, and so on. The fundamental framework for subsequent mathematical developments is based on velocity, body coordinates, and ground coordinates. The missile's centre of gravity (c. g.) serves as the point of origin for these coordinates. These coordinates define the horizontal plane within the ground coordinate system X_g−Z_g, and the Y_g axis complements the conventional right-handed system by extending perpendicularly. In body coordinates, the positive X_b axis corresponds to the roll-axis and aligns with the missile's centreline. The pitch axis is denoted by the positive Z_b axis, which is perpendicular to the X_b axis on the horizontal plane. The positive Y_b axis signifies the yaw axis and extends upward. The body axis system is co-moving and remains fixed with the missile. The direction of the missile's velocity (V_m), which corresponds to the direction in which the missile is traveling, is indicated by X_V in the velocity coordinate system. A typical right-handed coordinate system is supplemented with the Z_V axis [15, 16]. The X-Y plane represents the yaw plane, the Y-Z plane represents the pitch plane, and the X-Z plane represents the roll plane. During attitude angles (Ψ, Φ, Y), the ground coordinate and body coordinate are interlinked. Meanwhile, during angles (θ, σ), the ground coordinate and velocity coordinate are interconnected. In the pitch plane, during the angle of attack (α), and in the yaw plane, during the sideslip angle (β), the velocity coordinate system is associated with the body frame. Figure 1 illustrates the angles between various coordinate systems. A six-DOF missile is governed by six kinematic equations (three for rotational motion and three for translational motion) as well as six dynamic equations (three for rotational motion and three for translational motion) [17].

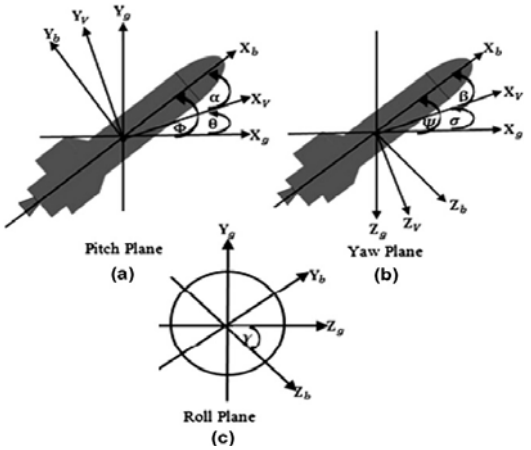

Fig. 1. Angles among coordinate systems

The equations for the six-DOF of the missile are derived as follows:

(1) $$F_x = m\dot{V}_m$$

(2) $$F_y = mV_m\dot{\theta}$$

(3) $$F_z = -mV_m\, cos(\theta)\, \dot{\sigma}$$

(4) $$M_x = I_x\dot{\omega}_x - \left(I_y - I_z\right)\omega_y\,\omega_z$$

(5) $$M_y = I_y\dot{\omega}_y - (I_z - I_x)\,\omega_z\,\omega_x$$

(6) $$M_z = I_z\dot{\omega}_z - \left(I_x - I_y\right)\omega_x\,\omega_y$$

(7) $$\dot{X} = V_m\, cos(\theta)\, cos(\sigma)$$

(8) $$\dot{Y} = V_m\, sin(\theta)$$

(9) $$\dot{Z} = -V_m\, cos(\theta)\, sin(\sigma)$$

(10) $$\dot{\Psi} = (\omega_y\, cos(\Upsilon) - \omega_z\, sin(\Upsilon))/\, cos(\Phi)$$

(11) $$\dot{\Phi} = \omega_y\, sin(\Upsilon) + \omega_z\, cos(\Upsilon)$$

(12) $$\dot{\Upsilon} = \omega_x - tan(\Phi)(\omega_y\, cos(\Upsilon) - \omega_z\, sin(\Upsilon))$$

(13) $$\dot{\alpha} = \dot{\Phi} - \dot{\theta}$$

(14) $$\dot{\beta} = \dot{\Psi} - \dot{\sigma}$$

where: M_x, M_y, M_z – moments represented in body coordinates [N·m]; I_x, I_y, I_z – moments of inertia in body coordinates [kg·m²]; $\omega_x, \omega_y, \omega_z$ – angular velocities in body coordinates [rad/sec]; F_x, F_y, F_z – components of forces represented in velocity coordinates [N]; *X* – the missile's range [m]; *Z* – horizontal displacement [m]; Y – the altitude [m]; *m* – the mass [kg].

The following equations calculate the moments and forces resulting from gravity, aerodynamics, and thrust acting on the missile [18, 19]:

(15) $$F_x = T\, cos(\alpha - \delta_\alpha)\, cos(\beta - \delta_\beta) - QS\big(C_{x0} + C_x(\alpha^2 + \quad + \beta^2)\big) - mg\ sin(\theta)$$

(16) $$F_y = T\, sin(\alpha - \delta_\alpha) + QSC_y\alpha - mg\ cos(\theta)$$

(17) $$F_z = -T\, cos(\alpha - \delta_\alpha)\, sin(\beta - \delta_\beta) - QSC_z\beta$$

(18) $$M_x = DQSm_{x0}\frac{\omega_x D}{2V_m}$$

(19) $$M_y = -T\, cos(\delta_\alpha)\, sin\big(\delta_\beta\big)X_{cg} + DQS\left(m_{y\beta}\beta + + m_{y0}\,\frac{\omega_y D}{V_m}\right)$$

(20) $$M_z = T\, sin(\delta_\alpha)X_{cg} + DQS\left(m_{z\alpha}\alpha + m_{z0}\,\frac{\omega_z D}{V_m}\right)$$

where: $m_{x0}, m_{y\beta}, m_{y0}, m_{z\alpha}, m_{z0}$ – aerodynamic moment coefficients [dimensionless]; $C_x,\ C_{x0}, C_y,\ C_z$ – aerodynamic force coefficients [dimensionless]; *D* – the maximum cross-section diameter [m]; *S* – the reference area [m²]; *Q* – the dynamic pressure[kg/m.sec^2]; δ_β – the yaw nozzle deflection angle [°]; δ_α – the pitch nozzle deflection angle [°]; *T* – the thrust force [N]; X_{cg} – the distance between the nozzle and the centre of gravity (c.g) [m]; g – the constant acceleration due to gravity, 9.81 [m/sec^2[.

The attitude control structure excludes the yaw and roll channels, focusing solely on the pitch channel within the X-Y plane. The following equations represent the nonlinear motion dynamics in the pitch direction [20, 21]:

(21) $$\dot{\Phi} = \omega_z$$

(22) $$\dot{\alpha} = \omega_z - \frac{F_y}{mV_m} = -\frac{QSC_y}{mV_m}\alpha - \frac{T}{mV_m}sin(\alpha - \delta_\alpha) + \omega_z + + \frac{g}{V_m}cos(\theta)$$

(23) $$\dot{\omega}_z = \frac{M_z}{I_z} = \frac{QSDm_{z\alpha}}{I_z}\alpha + \frac{QSD^2m_{z0}}{I_zV_m}\omega_z + \frac{TX_{cg}}{I_z}sin(\delta_\alpha)$$

Figure 2 illustrates the block diagram for pitch angle attitude control. The pitch nonlinear equations of motion, ranging from equation (21) to equation (23), can be approximated (for small angles, where sin(*x*) ≈ *x* and cos(*x*) ≈ 1) to obtain an LTV form as follows:

(24) $$\dot{\Phi} = \omega_z$$

(25) $$\dot{\alpha} = -\frac{T+QSC_y}{mV_m}\alpha + \omega_z + \frac{T}{mV_m}\delta_\alpha + \frac{g}{V_m}$$

(26) $$\dot{\omega}_z = \frac{QSDm_{z\alpha}}{I_z}\alpha + \frac{QSD^2m_{z0}}{I_zV_m}\omega_z + \frac{TX_{cg}}{I_z}\delta_\alpha$$

where the characteristics vary over time, the state space equations are as follows:

(27) $$\begin{bmatrix}\dot{\alpha}\\ \dot{\omega}_z\end{bmatrix} = \begin{bmatrix}-\frac{T+QSC_y}{mV_m} & 1\\ \frac{QSDm_{z\alpha}}{I_z} & \frac{QSD^2m_{z0}}{I_zV_m}\end{bmatrix}\begin{bmatrix}\alpha\\ \omega_z\end{bmatrix} + \begin{bmatrix}\frac{T}{mV_m}\\ \frac{TX_{cg}}{I_z}\end{bmatrix}\delta_\alpha + \begin{bmatrix}\frac{g}{V_m}\\ 0\end{bmatrix}$$

(28) $$\omega_z = \begin{bmatrix}0 & 1\end{bmatrix}\begin{bmatrix}\alpha\\ \omega_z\end{bmatrix}$$

(29) $$\Phi = \frac{1}{s}\omega_z$$

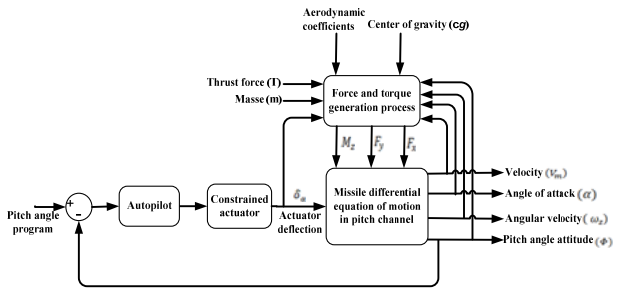

Fig. 2. Pitch angle attitude control block diagram

Methodology of nonlinear free body model

PID controller design

To ensure that the closed-loop system complies with the specified tracking constraints, PID controllers are designed, incorporating actuator chains. The PID controller's adjustable gains consist of k_i (integral gain), k_p (proportional gain), and k_d (derivative gain) [22]. The adjustable PID gains, along with actuator constraints, are achieved using the Nonlinear Control Design (NCD) blocks from Simulink's design optimization toolbox in Matlab. A detailed explanation of Simulink design optimization can be found in references [23, 24].

TVLQR design

The well-recognized concept of Linear Quadratic Regulation (LQR) is adapted to incorporate the framework of nonlinear control principles and nonlinear models. The TVLQR method simplifies complex and time-consuming calculations, leading to the development of more concise control algorithms suitable for integration into a missile's onboard computer [12]. The state-space LTV model for the system is represented as follows:

(30) $$\dot{x}(t) = B(t)u(t) + A(t)x(t)$$

The following optimal control law is satisfied by designing the state feedback matrix *K(t):*

(31) $$u(t) = -K(t)x(t)$$

To decrease the following cost function:

(32) $$J = \int_0^\infty (x^T Qx + u^T Ru)dt$$

where: $x \in \mathbb{R}^n$, control law $u \in \mathbb{R}^m$, $B \in \mathbb{R}^{mxn}$, weight matrixes $Q \in \mathbb{R}^{nxn}$, and $R \in \mathbb{R}^{mxm}$. Matrix Q is positive-definite or semi-definite ($Q = Q^T \geq 0$), and R is a positive-definite matrix ($R = R^T > 0$).

Equation (31) presents the linear control law. By identifying the undefined elements of matrix *K*, the cost function is minimized to determine the optimal control law $u(t)$ at the initial state $x(0)$. The state feedback gain matrix is obtained by solving the optimization problem as follows [25]:

(33) $$K(t) = R^{-1}B^T(t)P(t)$$

where: $P(t)$ is a positive-definite matrix ($P(t) = P^T(t) > 0$), and it is obtained through real-time solution of the Riccati equation, as demonstrated:

(34) $$A^T(t)P(t) + P(t)A(t) - P(t)B(t)R^{-1}B^T(t)P(t) + Q = 0$$

Through online solving of the state-space equations (27-29) and the Riccati equation (34), where:

(35) $$P = \begin{bmatrix}p_{11} & p_{12}\\ p_{12} & p_{22}\end{bmatrix}$$

(36) $$R = r$$

(37) $$Q = \begin{bmatrix}q_{11} & 0\\ 0 & q_{22}\end{bmatrix}$$

(38) $$A = \begin{bmatrix}a_{11} & a_{12}\\ a_{12} & a_{22}\end{bmatrix}$$

(39) $$B = \begin{bmatrix}b_1\\ b_2\end{bmatrix}$$

The parameters $q_{11}, q_{22}, \text{and } r$ are adjustable parameters tuned using Simulink Design Optimization, as detailed in [26]. By substituting equations (35-39) into equations:

(40) $$\begin{bmatrix}a_{11} & a_{21}\\ a_{12} & a_{22}\end{bmatrix}\begin{bmatrix}p_{11} & p_{12}\\ p_{12} & p_{22}\end{bmatrix} + \begin{bmatrix}p_{11} & p_{12}\\ p_{12} & p_{22}\end{bmatrix}\begin{bmatrix}a_{11} & a_{12}\\ a_{21} & a_{22}\end{bmatrix} - \frac{1}{r}\begin{bmatrix}p_{11} & p_{12}\\ p_{12} & p_{22}\end{bmatrix}\begin{bmatrix}b_1\\ b_2\end{bmatrix}\begin{bmatrix}b_1 & b_2\end{bmatrix}\begin{bmatrix}p_{11} & p_{12}\\ p_{12} & p_{22}\end{bmatrix} + \begin{bmatrix}q_{11} & 0\\ 0 & q_{22}\end{bmatrix} = 0$$

(41) $$q_{11} + 2a_{11}p_{11} + 2a_{21}p_{12} - \frac{1}{r}(b_1^2p_{11}^2 + 2b_1b_2p_{11}p_{12} + b_2^2p_{12}^2) = 0$$

(42) $$q_{22} + 2a_{22}p_{22} + 2a_{12}p_{12} - \frac{1}{r}(b_2^2p_{22}^2 + 2b_1b_2p_{22}p_{12} + b_1^2p_{12}^2) = 0$$

(43) $$a_{11}p_{12} + a_{22}p_{12} + a_{12}p_{11} + a_{21}p_{22} - \frac{1}{r}(b_1^2p_{11}p_{12} + b_1b_2p_{12}^2 + b_1b_2p_{11}p_{22} + b_2^2p_{22}p_{12}) = 0$$

Solving equations (41-43) yields the following equations:

(44) $$p_{11} = \frac{1}{b_1^2}\left(a_{11}r - b_1b_2p_{12} \pm \sqrt{r(a_{11}^2r + b_1^2q_{11} + 2a_{21}p_{12}b_1^2 - 2a_{11}p_{12}b_1b_2)}\right)$$

(45) $$p_{22} = \frac{1}{b_2^2}\left(a_{22}r - b_1b_2p_{12} \pm \sqrt{r(a_{22}^2r + b_2^2q_{22} + 2a_{12}p_{12}b_2^2 - 2a_{22}p_{12}b_1b_2)}\right)$$

(46) $$p_{12} = \frac{1}{2b_1b_2}\left((a_{11} + a_{22})r - b_1^2p_{11} - b_2^2p_{22} \pm \sqrt{x}\right)$$

The solution to the Riccati equation (34) at each time step is presented in equations (44) to (46). Equation (33) calculates the state feedback gain as follows:

(47) $$K = [k_1 \quad k_2] = \frac{1}{r}[b_1 \quad b_2]\begin{bmatrix}p_{11} & p_{12}\\ p_{12} & p_{22}\end{bmatrix} = \frac{1}{r}[b_1p_{11} + b_2p_{12} \quad b_1p_{12} + b_2p_{22}]$$

(48) $$k_1 = \frac{1}{r}(b_1p_{11} + b_2p_{12})$$

(49) $$k_2 = \frac{1}{r}(b_1p_{12} + b_2p_{22})$$

Equation (31) is used to compute the optimal control law.

(50) $$\delta_\alpha = -[k_1 \quad k_2]\begin{bmatrix}\alpha \\ \omega_z\end{bmatrix} = -(k_1\alpha + k_2\omega_z)$$

The closed-loop state feedback gain is given by:

(51) $$\begin{bmatrix}\dot{\alpha} \\ \dot{\omega}_z\end{bmatrix} = A_m\begin{bmatrix}\alpha \\ \omega_z\end{bmatrix}$$

(52) $$A_m = A - BK = \begin{bmatrix}a_{11} - b_1k_1 & a_{12} - b_1k_2 \\ a_{21} - b_2k_1 & a_{22} - b_2k_2\end{bmatrix}$$

TVLQR optimal controller was implemented to obtain a time-varying state feedback gain through the online solution of the Riccati equation (34). The results obtained from the nonlinear flight body model with TVLQR control will be compared with those from the nonlinear flight body model utilizing classical PID control [27, 28].

Model description

The missile's solid propellant thrust can be divided into two phases:

1. Boost phase: During the initial 0 to 5.8 seconds, the thrust force reaches its maximum level.
2. Sustain phase: Between 5.8 and 25 seconds, the thrust force decreases to its minimum value.

It is important to note that the pitch actuator deflection (δ_α) is limited to a range of ±22.9° (±0.4 rad). The thrust force curve is depicted in Figure 3.

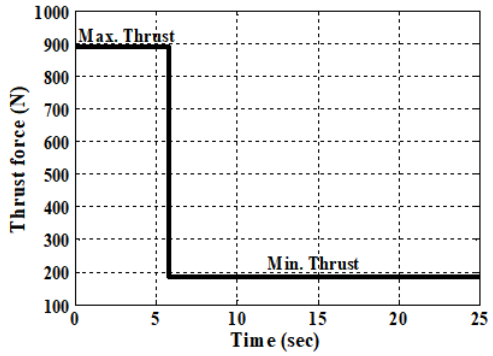

Fig. 3. Thrust force curve

The linear time-varying model (LTV), with varying parameters (A, B) over time, is formulated by approximating the nonlinear model within the pitch channel.

PID and TVLQR controllers design

The PID controller's gains, including kd (derivative gain), ki (integral gain), and kp (proportional gain), require adjustment. In Matlab, the Simulink Design Optimization software is employed for optimizing the PID gains while considering the actuator chain. The PID controller settings for the pitch channels are presented in Table 1.

Table 1. The optimized PID parameter controller for pitch channel

k_p	k_i	k_d
20.47	50.8965	4.709

Table 2. The tuned matrixes Q, R of TVLQR and integral gain for pitch channel

q_{11}	q_{22}	r	k_f
0	1319.4	0.1849	871.4

The TVLQR controller is designed for the pitch channel of the nonlinear model. The state feedback gain, K, in equation (47), is calculated online through the Riccati equation (34), and the matrices R and Q in equations (36) and (37) are adjusted using Simulink Design Optimization. As the matrices A and B of the LTV model change with time, the state feedback gain, K, also varies dynamically. To drive the error to zero, the error signal is integrated with a gain, kf. The parameters for the TVLQR matrix Q and R, as well as the integral gain kf for the pitch channel, are presented in Table 2.

Results

Pitch angle response

The initial value of the step unit reference signal is set at 40° (0.698 rad), and within the first second, it transitions to a final value of 41° (0.716 rad). Utilizing this reference signal, both the pitch channel PID and TVLQR controllers are implem. Figure 4 illustrates the pitch angle of the nonlinear model and the LTV model with the PID controller, highlighting that the LTV model closely approximates the behavior of the nonlinear model.

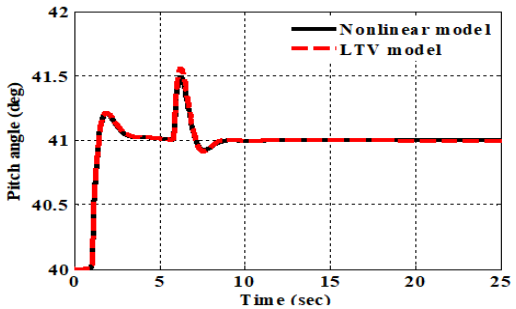

Fig. 4. Pitch angle responses for nonlinear and LTV with PID controller

Figure 5 displays the terms of the state feedback gain as described in equations (48) and (49). Figure 6 displays the nonlinear pitch responses for both TVLQR and PID controllers with a pitch step unit reference signal. The figure illustrates the plant's output signal, which is the pitch angle Φ(t), the pitch error represented as the difference between pitch demand and pitch angle, denoted as e(t), and the input signal to the plant, which is the pitch actuator deflection $\delta_\alpha(t)$.

Wind effect

To assess the impact of wind, the pitch error and actuator deflection are examined. Wind velocity is introduced in the opposite direction to the missile's velocity (Vm). Figure 7 how the TVLQR controller manages the effects of wind on pitch responses.

Dynamics uncertainty

The presence of uncertainties has a detrimental effect on the closed-loop system's capacity to track aerodynamic coefficients. In the case of the six-DOF nonlinear missile, a TVLQR controller is devised to address uncertainties in aerodynamic forces and moments [29]. It is possible to examine how the pitch channel autopilot responds to different levels of dynamic uncertainty.

Figure 8 illustrates the pitch responses for PID controllers under varying degrees of dynamic uncertainty. Notably, when the pitch angle exceeds control limits, and the pitch actuator deflection saturates during the sustain phase, a PID controller proves inadequate in the face of a 50% dynamic uncertainty. Figure 9 presents the pitch responses for TVLQR controller under dynamic uncertainty percentages.

The TVLQR controller is capable of effectively managing different dynamic uncertainty percentages. Figure 10 illustrates the terms of the state feedback gain for various levels of dynamic uncertainty.

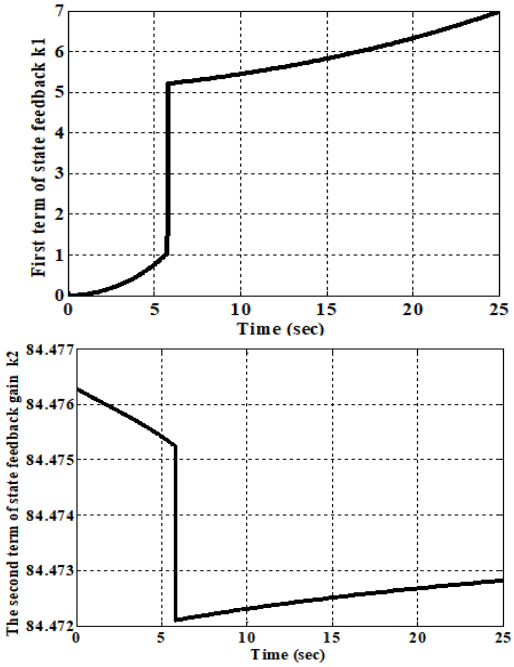

Fig. 5. The terms of state feedback gain

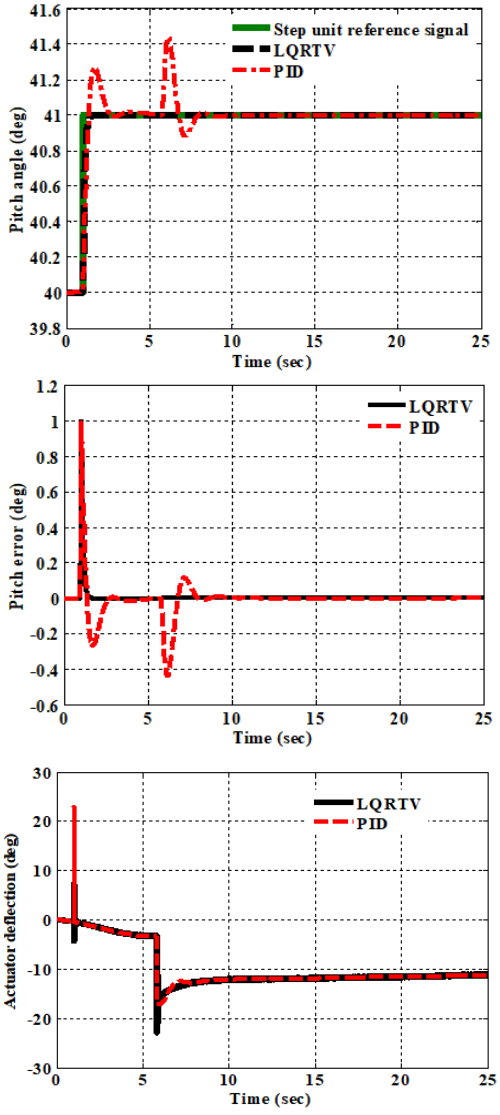

Fig. 6. Pitch responses

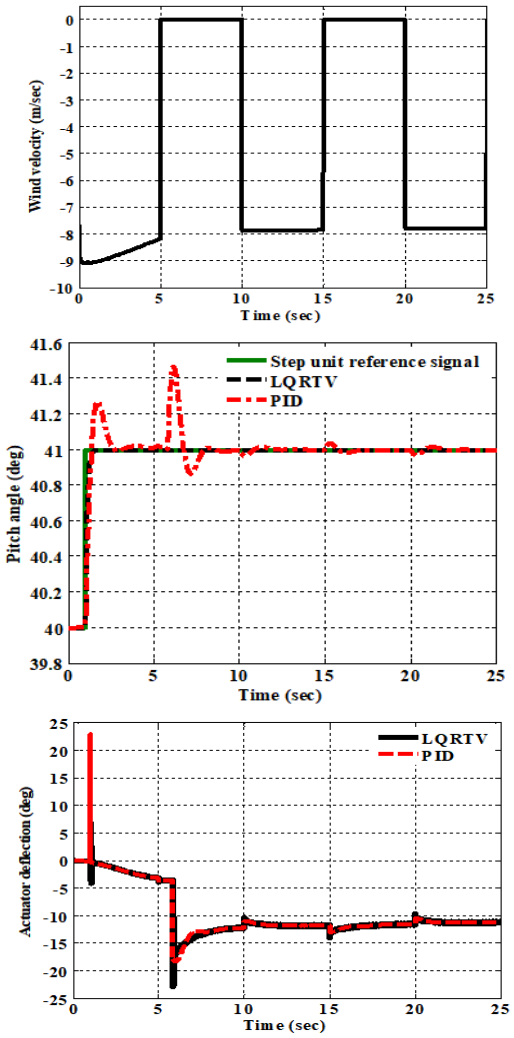

Fig. 7. Pitch responses with wind effect

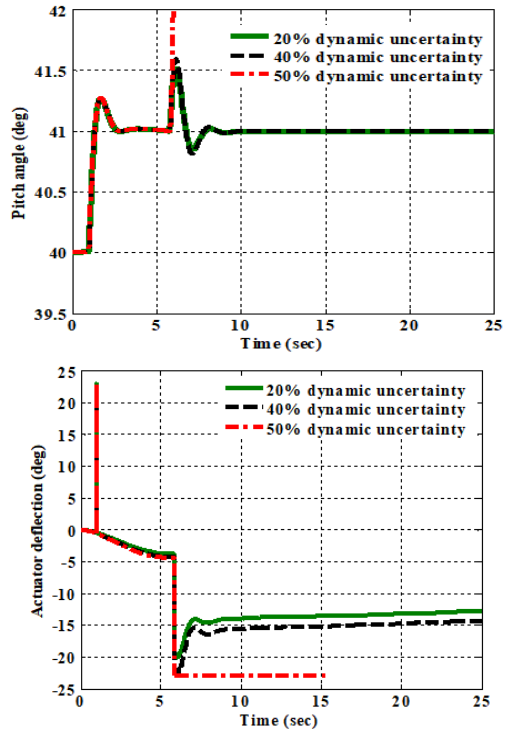

Fig. 8. Pitch responses for PID controller with different dynamic uncertainty percentage

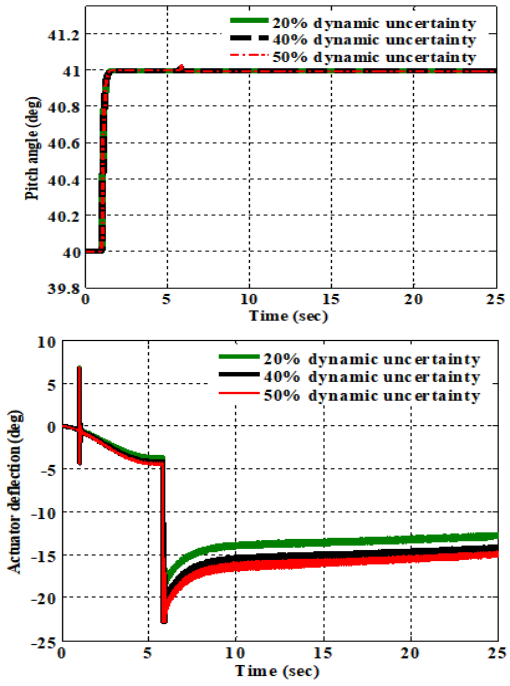

Fig. 9. Pitch responses for TVLQR controller with different dynamic uncertainty percentages

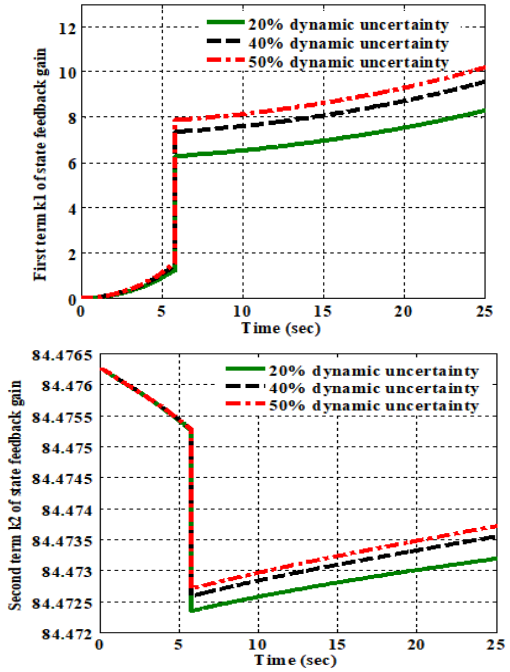

Fig. 10. The terms of state feedback with different dynamic uncertainty percentage

Actuator uncertainty

The following equation describes the relationship for actuator uncertainty, representing a disturbance affecting the actuator deflection (plant input):

(53) $$u = \delta_\alpha + d$$

(54) $$d = \delta_\alpha \left(1 - \frac{1}{\lambda}\right)$$

where: λ represents the uncertainty parameter, which equals 1 when there is no uncertainty (d = 0). For instance, if the actuator uncertainty is 20%, then λ would be calculated as follows: $\lambda = 1 - 0.2 = 0.8$.

Figure 11 displays the pitch responses for the PID controller under varying actuator uncertainty percentages. Notably, the PID controller struggles to handle a 45% actuator uncertainty. During the sustain phase, the pitch actuator deflection becomes saturated, and the pitch angle becomes uncontrollable. Figure 12 illustrates the pitch responses for the TVLQR controller with different actuator uncertainty percentages. The TVLQR controller demonstrates its capability to effectively manage various levels of dynamic uncertainty

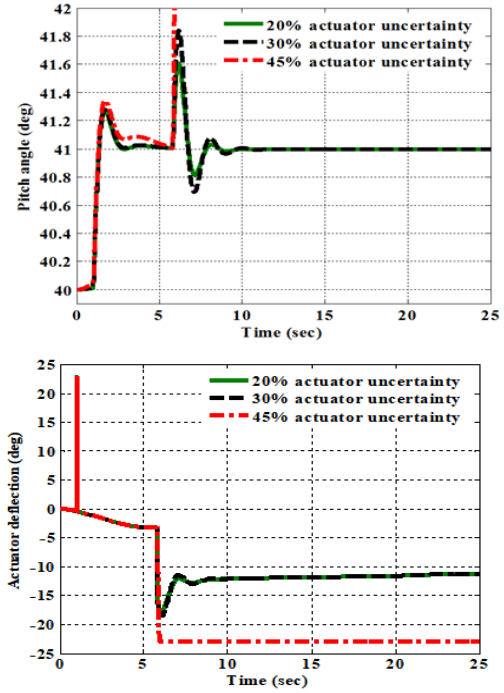

Fig. 11. Pitch responses for PID controller with different actuator uncertainty percentage

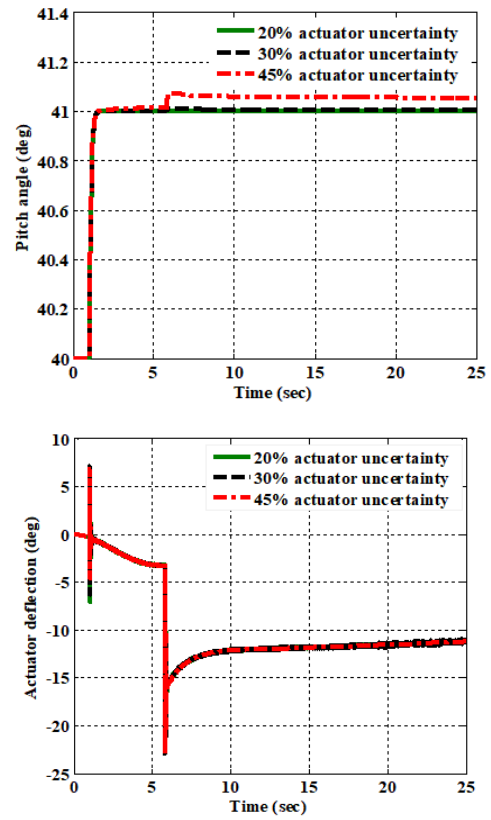

Fig. 12. Pitch responses for TVLQR controller with different actuator uncertainty

Conclusions

In this study the optimal tuning parameters for both PID and TVLQR controllers are determined and compared using Simulink design optimization. The LTV model exhibits the closest resemblance to the nonlinear model for the six-DOF missile. The state feedback gains of the TVLQR controller change over time due to online calculations involving the Riccati Equation. The TVLQR optimal control, designed using the LTV model, was implemented on the nonlinear flying body in the pitch channel. A comparison of the responses between PID and TVLQR controllers reveals that both controllers effectively track the step unit reference signal in terms of pitch angle. However, TVLQR stands out as it provides the most desirable tracking with no overshoot during the first and 5.8 seconds. Moreover, TVLQR exhibits no steady-state error after the initial second, in contrast to PID where a steady-state error was observed.

The actuator deflection response in TVLQR surpasses that of the PID controller, where the actuator remains unsaturated within the first second. Additionally, TVLQR's response remains unaffected by the wind effect. TVLQR demonstrates its capability to handle 50% dynamic uncertainty and 45% actuator uncertainty, while the PID controller cannot achieve.

Acknowledgements: *This article was supported by the Lublin University of Technology (Grant No. FD-20/IS-6/002).*

Authors: *Dr Mohamed Fawzy, Department of Electrical Engineering, Factly of Engineering, MTI University, Cairo, Egypt, e-mail: Mohamed.fawzy@eng.mti.edu.eg; Dr Hani Attar, Department of Energy Engineering, Zarqa University, Jordan, e-mail: Hattar@zu.edu.jo; Dr Ayman Amer, Department of Energy Engineering, Zarqa University, Jordan, e-mails: Aamer@zu.edu.jo; Prof. Sameh Alsaqoor, Department of Mechanical Engineering, Tafila Technical University, P.O. Box 179, 66110, Tafila, Jordan, e-mail: sameh@wp.pl; Prof. Ali Alahmer, Department of Mechanical Engineering, Tuskegee University, Tuskegee, AL 36088, United States of America; Prof. Gabriel Borowski, Faculty of Environmental Engineering, Lublin University of Technology, ul. Nadbystrzycka 40B, 20-618 Lublin, Poland, e-mail: g.borowski@pollub.pl; Dr Ahmed A.A. Solyman, School of Computing, Engineering and Built Environment, Glasgow Caledonian University, Glasgow, UK, e-mail: ahmed.solyman@gcu.ac.uk; Dr Samer As'ad, Renewable Energy Engineering Department, Middle East University, Jordan, Dr Ramy Said Agieb, School of Computing, Engineering and Built Environment, Glasgow Caledonian University, Glasgow, UK, e-mail: ahmed.solyman@gcu.ac.uk*

REFERENCES

[1] Aboelela M.A., Ahmed M.F., Dorrah H.T., Design of aerospace control systems using fractional PID controller. *Journal of Advanced Research,* 3 (2012), 225–232. https://doi.org/ 10.1016/j.jare.2011.07.003
[2] Draper C., Guidance is forever. *Navigation,* 18 (1971), 26–50.
[3] Spearman M.L., Historical development of worldwide guided missiles: NASA Langley Research Center, 1983.
[4] Elbes M., Alzubi S., Kanan T., Al-Fuqaha A., Hawashin B. A survey on particle swarm optimization with emphasis on engineering and network applications. *Evolutionary Intelligence*, 12 (2019), 113–129. https://doi.org/10.1007/s12065-019-00210-z
[5] Westrum R., Sidewinder: creative missile development at China Lake: Naval Institute Press, 2013.
[6] Adeli H., Kim H., Wavelet-hybrid feedback-least mean square algorithm for robust control of structures, *Journal of Structural Engineering,* 130 (2004), 128–137. https://doi.org/10.1061/(ASCE)
0733-9445(2004)130:1(128)
[7] Agha A., Attar H., Luhach A.K., Optimized economic loading of distribution transformers using minimum energy loss computing. *Mathematical Problems in Engineering*, (2021), Article ID 8081212. https://doi.org/10.1155/2021/8081212
[8] Campa G., Algebraic riccati equation solution in simulink via c+ fortran. *Matlab Central File Exchange,* 2001.
[9] Zhou K., Doyle J.C., Glover K., Robust and optimal control. Prentice Hall New Jersey, 40 (1996).
[10] Wu W.-H., Chase J.G., Smith H.A., Inclusion of forcing function effects in optimal structural control. In: Proceedings of the First World Conference on Struct. Control. *TP2-22-TP2-31* (1994).
[11] Ayman A., Hani A., Audih A., Mohammad K.R., Maximizing electrical power saving using capacitors optimal placement. *Recent Advances in Electrical & Electronic Engineering*; 13 (2020), 7. https://dx.doi.org/10.2174/2352096513666200212103205
[12] Bigot P., Souza L., Investigation of the state dependent Riccati equation (SDRE) adaptive control advantages for controlling nonlinear systems as a flexible rotatory beam. *International Journal of Systems Applications, Engineering and Development.,* 8, (2014).
[13] de Souza L.C.G., Design of satellite control system using optimal nonlinear theory. *Mechanics Based Design of Structures and Machines,* 34 (2006), 351-364. https://doi.org/10.1080/153977306 01044853
[14] Fawzy M., Aboelela M., El Rhman O.A., Dorrah H., Design of missile control system using model predictive control. *Online Journal on Computer Science and Information Technology,* 1 (2011), 3, 64–70.
[15] Abu Qudeiri J.E., Saleh A., Ziout A., Mourad A.-H.I., Abidi M.H., Elkaseer A., Advanced electric discharge machining of stainless steels: Assessment of the state of the art, gaps and future prospect. *Materials*,12 (2019), 907. https://doi.org/10.3390/ma120 60907
[16] Siouris G.M., Missile guidance and control systems. Books24x7.com, 2005.
[17] Ashish T., Modern control design with Matlab and simulink. Indian Institute of Technology, Kanpur, India, John Wiley & Sons (2002).
[18] Siouris G.M., Missile guidance and control systems. Springer Science & Business Media, 2004.
[19] Salem N., Study on the effect of vibratory stress relief on the quality of gravity die casting-theory and justifications. In: Proceedings of the 5th International Conference on Advanced Materials, Mechanics and Structural Engineering (5th AMMSE 2018) Seoul, Korea, https://iopscience.iop.org/article/10.1088/1757-899X/473/1/012041/pdf,
[20] Stevens B.L., Lewis F.L., Johnson E.N., Aircraft control and simulation: dynamics, controls design, and autonomous systems. John Wiley & Sons, 2015.
[21] Cook M.V., Flight dynamics principles: A linear systems approach to aircraft stability and control. Butterworth-Heinemann, 2012.
[22] Salem N., Hussei M.A., Hasan N., Ali A.S., Motion control of ultrasound probe based on master-slave robotic system for medical ultrasound applications. *International Journal of Advanced Science and Technology*, 28 (2019), 18, 749–759, http://sersc.org/journals/index.php/IJAST/article/view/2793,
[23] Tyagi A.K., MATLAB and SIMULINK for Engineers: Oxford University Press, 2012.
[24] MathWorks, MATLAB: the language of technical computing. Desktop tools and development environment, version 7.10.0 vol. 9: MathWorks, 2010.
[25] Burns R., Advanced control engineering. Butterworth-Heinemann, 2001.
[26] Tyagi A.K., MATLAB and SIMULINK for Engineers: Oxford University Press, 2012.
[27] Yuan L., Cui J., Pan M., Liu Y., Design of aerodynamics missile controller based on adaptive fuzzy PID. In: Measurement, Information and Control, International Conference on (2012), 712–716.
[28] Siouris G.M., Missile guidance and control systems. Springer Science & Business Media, 2004.
[29] Saadia H., Awan A.U., Khan K.F.A., Liaquat M., Waheed S., Adaptive control of air-to-air missile using multilayer NN feedforward and RISE feedback terms. In: 10th Asian Control Conference, 2015, 1–8.